

# Discovering Ultra High Energy Neutrinos by Horizontal and Upward Air-Shower: First evidences in Terrestrial Gamma Flashes

D. Fargion<sup>1,2</sup>

Physics Department, Rome University 1

"La Sapienza", INFN, P.le A. Moro 2, 00185 Roma, Italy.

Daniele.Fargion@roma1.infn.it

## ABSTRACT

Ultra high energy neutrinos UHE, and  $\nu_e$  at PeV and higher energy may induce air-showers whose detectability is million to billion times amplified by their secondaries. We considered UHE  $\nu$  and UHE  $\nu_e$  interactions beyond mountains as a source of such horizontal amplified air-showers. We also consider upward UHE  $\nu$  interaction on Earth crust at horizon and their UHE air-showers beam ing toward high mountains detectors. We show their detectability. We notice that such rare upward air-shower may hit even nearby satellite and ash them by short diluted burst at the edge of Gamma Ray Observatory detection threshold. We identify these events with recent (1994) discovered (BATSE) Terrestrial Gamma Flashes and we claim their probable UHE - UHE origin. From these data approximated UHE flux and mass lower bound are derived. Known X  $\sim$  TeV active galactic and extragalactic sources have been identified in most TGF arrival directions. Partial TGF Galactic signature is also manifest.

Subject headings: Neutrino { UHE cosmic rays { Tau lepton

## 1. Introduction

Ultra high energy air-showers are a powerful tool in discovering primary ultra high energy (UHE) neutrinos. The UHE neutrino interaction with nuclear matter, as well as the  $\nu_e$  interaction with matter electron at W G lashow peak, their UHE tau production and the consequent tau traces inside matter and outside in air may lead, by final decay in flight, to rich amplified air-shower traces. These huge air-shower signals being at least million to billion times more abundant (B. Rossi 1964) than the original and unique UHE track in matter are much easier to be detected. Experimental set up described in this paper may reduce or avoid common cosmic ray background noise leading to a meaningful UHE neutrino dis-

cover in short (one year) time.

The source of UHE, since Super Kamiokande evidence of neutrino flavour mixing, must be as abundant as muon ones. Moreover the expected signals, by their secondary tau tracks, in underground Km<sup>3</sup> detectors at highest cosmic ray energy window  $1.7 \cdot 10^{10}$  eV  $> E > 1.6 \cdot 10^{10}$  eV, must exceed the corresponding (or muonic) ones, making UHE above 0.1 EeV the most probable UHE signal. Indeed, the Lorentz-boosted tau range length grows (linearly) above muon range, for  $E > 1.6 \cdot 10^{10}$  eV. The tau track reaches its maximum extension, bounded not by pair production, but by nuclear electro-weak interactions,  $R_{\max} \sim 191$  Km, at energy  $E \sim 3.8 \cdot 10^{10}$  eV. At this peak the tau range is nearly 20 times longer than the corresponding muon range (at the same energy) implying, for comparable fluxes, a ratio 20 times larger in

<sup>1</sup> INFN, Roma1, Italy

<sup>2</sup> Technion Institute, Eng. Faculty, Haifa, Israel

over detection probability. This dominance, may lead (at present most abundant UHE models) to a few rare spectacular event a year (if avorm mixing occurs) preferentially in horizontal plane in underground  $K m^3$  detectors. The Earth opacity at those UHE regimes at large nadir angles (nearly horizontal, few degree upward direction) is exponentially different for UHE muons respect to tau at GZK limits, making their flux ratio severely suppressed. This signal may be hardly noticed in  $K m^3$  detectors, but they must be recorded in fine tuned directional upward air showers.

Indeed because of the tau air-shower prolific behaviour, we, first, suggest new kind of UHE neutrino detectors located in deep hole (Kimberly mine) or deep valley in front of high mountains chains to discover their peculiar horizontal UHE

and decay beyond a thick mountain and their final induced air showers. The mountain act as a triple filter:

- as a screen of undesirable horizontal Ultra High Energy Cosmic Rays (UHECR) (electromagnetic shower, secondary Cherenkov photons and muons),
- as a calorimeter for UHE  $\tau$ ,  $\nu_e$ , and  $\bar{\nu}_e$ ,
- as a distance meter correlating tau relativistic track and birth and its air-shower opening distance from the mountain with UHE tau original energy. Indeed because of the different neutrino interactions with energy and avors it will be possible to estimate, by stereoscopic, directional and time structure signature, the spatial air-shower origination, the primary tau distance decay from the mountain (tens of meter for PeVs UHE  $\tau$  and nearly hundred meters and  $Km$ s for UHE  $\nu_e$ ,  $\bar{\nu}_e$ ), the consequent most probable original UHE tau range and energy. Additional energy calibration may be derived sampling shower intensities.

Secondly we suggest here to discover UHE  $\tau$ , by observing the upward tau air-shower arriving from hundred  $Km$  meters away (near horizontal edges) from high mountains, high balloons and satellites; such UHE tau created within a wide (tens thousands to millions square  $km^2$  wide and hundred meter depth in Earth crust) target would discover UHE  $\tau$ , neutrinos at PeV up to EeV energies and above, just within the mysterious GZK frontiers. The discovery will need capable gamma, op-

tical and muon bundle detectors within present technology.

Finally from the same highest mountains, balloons and near orbit satellite, looking more downward toward the Earth it is possible to discover more frequent but lower energetic astrophysical PeV - tens PeV UHE tau trace within small and large nadir angles, by their air-shower secondaries (Cherenkov lights, muons and gamma bursts).

These PeVs upward UHE tau may beam their air-showers and gamma secondaries to high altitudes toward existing satellites. We show that their signal is at the edge of detection of Compton Gamma Ray Observatory (CGRO), namely BATSE experiment. These signals are, very probably, already recorded in Terrestrial Gamma Flash. Their angular and directional distributions with galactic plane and their clustering toward known active sources (Galactic center, Crab, ..) are very suggestive for their UHE astrophysical origin.

### 1.1. The UHE $\tau$ , $\nu_e$ , and their UHE secondary

Ultra high energy astrophysical neutrino (UHE) from PeVs ( $\sim 10^{15}$  eV) up to ( $10^{18}$  eV) EeV and GZK cut off energies ( $\sim 10^{19}$  eV) might be traced by induced air showers and by their millions to hundred billions multiplicity in secondaries particles.

Indeed astrophysical PeVs UHE antineutrino electrons,  $\nu_e$ , near the Glashow  $W$  resonance peak,  $E_{\nu_e} = M_W^2 = 2m_e c^2 / 6:3 \cdot 10^6$  eV, (dominant over expected UHE PeV atmospheric neutrino signals), may be observable by their secondary horizontal

air showers originated by UHE chain reaction  $e + e^- \rightarrow W^- + \bar{W}^+$  inside the concrete rock of a high mountain. Also UHE  $\tau$ , at ( $10^{16}$  -  $10^{17}$  eV) would be observable if avor mixing  $\tau \rightarrow \nu_e$  take place as shown by Superkamiokande data.

The mountain and the air act as a clever multi filter:

- as a screen of undesirable horizontal UHECR (electromagnetic shower, secondary Cherenkov photons and muons),
- as a calorimeter for UHE  $\tau$ ,  $\nu_e$ , and  $\bar{\nu}_e$ ,
- as a distance meter target correlating birth place and its air-shower opening with its most probable energy,
- as an unique source, by tau hadronic shower-

ing, of horizontal and deep muon bundle source. The process is analogous to the Learned and Pakwasa (1995) "double bang" in neutrino detectors. The novelty of the present "one bang in" (the rock) - "one bang out" (the air) lays in the self-triggered explosive nature of decay in light and its consequent huge amplified air shower signal at a characteristic few Km s distance. Detectable horizontal gamma bursts (mainly bremsstrahlung photons) are one of the most abundant signal. The huge secondary air shower amplification (million-billions fold) make extremely easier the UHE discovery respect to a single underground or track. The PeV energy necessary to born such air showers are not ambiguous as a Km length track in a Km<sup>3</sup> volumes, whose identity may be associated also to secondary atmospheric (tens to hundred TeV) muons.

Screening by undesirable lateral or downward noisy cosmic rays or natural radiation is possible by directional and time clustering filter; therefore the induced  $e^+e^-$  air shower even in absence of  $\bar{e}e$  oscillation should be identified and detectable soon. Its unique  $e$  origin is marked by the peaked  $W$  resonance, and by the small mountain opacity and its high neutrino cross-section. Its identity is marked by the expected fine tuned PeV energy at  $W$  peak and the tau air-shower birth place near (a hundred meter) the mountain wall.

More copious ( $> 5$  times more) events by PeV up to tens PeV  $N$  interaction occur if oscillate in  $e$ . The UHE  $e$  are default and expected UHECR ( $\& 10^{16}$  eV) secondary products near AGN or microquasars by common photo-pion decay relics by optical photons nearby the source (PSRs, AGNs) ( $p^+e^-; n^+e^+; \bar{n}^+e^-; \bar{p}^+e^+$ ). In this case their source directionality is frozen and it is conserved.

These neutrino secondaries may be also very rare photo-pion products during the EeV CR propagation and interaction in the dimmed galactic lights. In this (rare) case they may lose their primordial source directionality. The  $e$  signal at Glashow resonance peak does not depend on any production or any avormixing. Therefore  $e$  UHE detection by a mountain screen is a necessary and unavoidable signal related to the existence of UHECR at  $10^{16}$  eV and photo-pion production. In addition to UHE  $e$  role at Glashow peak,

one has to note the peculiar behaviour of UHE tracks which are relativistically boosted (linearly with energy) longer and longer up to such lengths ( $L \& 5$  Km for  $E \& 10^{17}$  eV) comparable or exceeding the corresponding muon tracks  $L$  in matter, being  $L$  bounded by slow logarithmic law growth (with energy), at a few Km s, mainly by pair production losses. Because of higher mass and the pair production dependence approximately on  $m^2$  such electromagnetic losses are negligible for  $e$ .

Therefore neutrino tau ( $\tau$ ; at  $10^{17}$  eV energies or above) leave the longest traces in matter and they are the most detectable UHE neutrino signals in Km<sup>3</sup> detectors. Unfortunately tracks growth in rock reaches a maximal extension, because of the growth of  $N$  electro-weak nuclear interactions, at  $E \& 3.8 \cdot 10^{18}$  eV,  $L \& 191$  Km. This peak ranges are nearly twenty times longer than muon ones. For higher energies nuclear interactions bound and reduce the lengths.

These traces, up to energy  $E \& 10^{21}$  eV are nevertheless longer and therefore more detectable than muon ones; only at higher energies both avors should share comparable ( $L; L$ ) lengths, uniformed by common UHE electro-weak-nuclear interactions. Astrophysical UHE and  $\tau$  at energies  $E \& 10^{16} \cdot 10^{21}$  eV are difficult to be directly produced by  $p + p$  scattering, but they might be copiously converted by full avormixing

$\bar{e}e$ ,  $\bar{e}e$ , strongly required by recent Superkamiokande atmospheric neutrino asymmetries. Therefore UHE  $e$  and  $\tau$  may be converted and they may reach us from high energy galactic sources, as pulsars, SNRs, black holes or galactic SGRs microquasars, as well as from powerful extragalactic AGNs, quasars or GRBs, even for any small mass mixing, ( $m_{ij}^2 \& 10^4$  eV<sup>2</sup>) or any high (GZK) energy because of the large galactic (Kpc) and extreme cosmic (Mpc) distances:

$$L = 40 \text{ pc} \cdot \frac{E}{10^{20} \text{ eV}} \cdot \frac{m_{ij}^2}{(10^2 \text{ eV})^2} \quad (1)$$

Such UHE  $e$ , as well as the UHE  $\tau$  near a narrow energy resonant  $W$  peak ( $E_e = M_W^2 = 2m_e = 6.3 \cdot 10^{18}$  eV), may interact on Earth (the calorimeter) leading to UHE  $e$  which are mostly absorbed by the same planet.

However rare upward UHE  $\nu_e$ , born by  $\nu_e$  and nuclear (or rare  $\nu_e \bar{\nu}_e$  interactions near the upward earth surface), may escape outside on air where they may spontaneously decay triggering upward vertical, oblique or near horizontal air showers. The vertical ones (by small nadir angle) occur preferentially at low energies nearly transparent to the Earth ( $E_e = 10^{15} - 10^{16}$  eV). The oblique air showers whose arrival directions have large nadir angle, are related mainly to higher energy  $\nu_e$ , or nuclear interactions ( $E_e = 10^{17} - 10^{18}$  eV). Indeed these horizontal - upward UHE cross a smaller fraction of the Earth volume and consequently they suffer less absorption toward the horizon.

These oblique - vertical upward air showers, complementary to the PeVs  $\nu_e$  and PeVs and tens of PeVs  $\nu_e$ , leading to horizontal air showers beyond high mountains, should be discovered at best from large arrival distances corresponding to the longer tracks from high ( $\sim 10^5$  Km) mountain observatory hunting for secondaries shower Cherenkov lights, muon bundle and directional electron - gamma shower bursts from below toward the Earth. The maximum observational distances may reach  $110$  Km ( $h=K m^{\frac{1}{2}}$ ) toward the horizon, corresponding to a UHE energy  $2 \times 10^{16}$  eV ( $h=K m^{\frac{1}{2}}$ ). Therefore we propose to consider such upward shower nearly horizontal detection from high mountains to test this highest energy window almost "blind" to G-lashow UHE  $\nu_e$  fluxes. The comparison of upward showers with the horizontal tau showering beyond mountains, made up also (20%) by  $\nu_e$  at  $6:3 \times 10^{16}$  eV energy, would constrain and measure the neutrino flavor parameters.

The same tau upward air showers, observable from future balloons or dedicated satellites, UHE air showers born in a narrow energy window,  $10^{15} - 10^{16}$  eV.  $E_e = 5 \times 10^{16}$  eV may penetrate high altitude leaving rare beam upward gamma shower bursts whose sharp (hundreds sec) time structure and whose hard ( $\sim 10^5$  eV) spectra may hit near terrestrial satellites.

Here we claim that such gamma upward events originated by tau air showers produce gamma bursts at the edge of GRO-BATSE sensitivity threshold. In particular we argue that very probably such upward gamma events have been already detected since April 1991 as serendipitous sharp

( $\sim 10^{-3}$  sec) and hard ( $\sim 10^5$  eV) BATSE gamma triggers originated from the Earth and named consequently as Terrestrial Gamma Flash (TGF). However since 1994 (Fishman et al.) TGF understanding of presently known 75 records over nearly eight thousand BATSE triggers is based on an unexpected and mysterious high latitude lightning of geophysical nature (the so called "Sprites" or "Blue Jets").

We do not believe in that interpretation. We notice that among the 75 records only 47 are published in their details, while 28 TGF are still unpublished. While Blue Jets might be in principle triggered by upward tau air showers in the atmosphere (a giant "Wilson" room) we believe they are not themselves source of TGF. In particular their observed characteristic propagation velocity ( $\sim 100$  Km/s) from distances  $\sim 500$  Km, disagree with short TGF millisecond timing and would favor a characteristic TGF time of few seconds.

Moreover TGF data strongly disfavor by its hard spectra the terrestrial Sprites connection. On the contrary the expected UHE tau upward air showers (triggered by UHE  $\nu_e$  at energies  $10^{15} - 10^{17}$  eV) lead to a gamma burst flux, spectra, and time structure in agreement with the observed TGF ones and in reasonable agreement with the expected galactic - extragalactic UHE neutrino flux models and UHE neutrino experimental bounds, even considering the UHE neutrino Earth opacity. In addition time clustering of a few known TGFs, marked by their "repeater" nature or directional clustering (triplets) toward defined directions makes the extra-terrestrial connection very plausible. Moreover the same correlations of these clustered TGFs directions toward

- (1) well known and maximal powerful galactic and extra-galactic sources either at TeV, GeV - MeV, X band,
- (2) recent first anisotropy discovered on UHECR at EeV by AGASA,
- (3) the Milky Way Galactic Plane,

all these independent evidences support and make compelling the TGF identification as secondary gamma burst tail of UHE  $\nu_e$  induced upward air shower.

The present TGF - air-shower identification could not be produced by UHE  $\nu_e$  charged current resonant event at ( $E_e = M_W^2 = 2m_e = 6:3 \times 10^{16}$

eV), and therefore it stand for the UHE existence. Consequently it gives support to the Superkam iokande evidences for  $\pm$  avor mixing from far PSRs or AGNs sources toward the Earth.

The TGF-air-shower connection may be soon verified and reinforced (or partially mystified) by the prompt BATSE-GRO publishing of 28 missing TGFs data which probably hide additional directional imprint of UHE sources. Two main TeV sources, Mark 421 and Mark 501, absent in the 47 published TGF BATSE data, could be hidden in those unpublished events.

We notice that since two years the TGF rate is rare (3 event a year). We also notice that the variable satellite GRO height didn't play in the past any role in the TGF detection rate.

Nevertheless older BATSE trigger set up and threshold have shown a much proliferous (ten fold) sensitivity to TGF activity. Therefore the recovery of such a "hard" trigger (by channel 3 + 4 and low threshold at 4.5 as the very recent set up (4 February 2000)) may immediately amplify the BATSE sensitivity toward these upward gamma bursts, offering a wider sample (doubling present 75 events) in a quite short time (a couple of years). We remind that UHE interaction at PeV-EeV energies correspond to an invariant center of mass energy comparable or above future LHC accelerators, offering an additional powerful astrophysical high energy laboratory.

The upward air shower - TGF identification while opening a new UHE neutrino astronomy, offers a first "directional" UHECR tool (s are not bent by magnetic fields) and deeper (UHE s are weakly interacting particles nearly transparent to dense AGN or PSRs cores surrounding) views of most violent cosmic accelerators.

Finally the very possible origin of TGFs, better proved (or disproved) by near future experiment on fluxes (made beyond or above mountains) will finally test the  $\pm$  avor mixing. At the present the very probable source of TGFs and their probable partial galactic location infer a first lower bound on  $m$  ( $L < 4$  Kpc,  $m > 10^8$  eV<sup>2</sup>) and it offers a first direct test of the same existence of the last missing, yet unobserved, fundamental neutral lepton particle: and .

This article is structured as follows:

In the second section we discuss the main roles of neutrino in elementary particle and astrophysics. In particular we recall the neutrino mass role and the avor mixing.

In the third section we explain dominant role of UHE ( $E > 10^{17}$  eV) over UHE by their peculiar penetrability in Km<sup>3</sup> detectors and air showers.

In the following fourth section we briefly summarize the expected source and spectra of UHE . In the fifth section we reconsider the ee charged current interactions at resonant energies leading to W, whose decay may lead to ultrarelativistic .

The topic recall known ideas (as the double bang in Km<sup>3</sup>) and new proposals as the UHE air shower behind a mountain chain (Fargion, Aiello, Conversano 1999), to detect PeVs e and , N events. In this section the ranges are combined for all interactions, mainly in Km<sup>3</sup> detectors.

In the sixth section we consider the N ; N interactions at highest energy leading to upward air shower observable from above (mountains, balloons) and their expected rates and signal/noise signature.

In this last seventh section we also describe the consequences of UHE upward air showers into bursts. In particular we shall analyze the discover of TGF, their Sprite - Bubble Jet models, and their untenable connection to TGF .

We show the known 75 TGF data, the 47 published ones in astronomical coordinate and their remarkable correlation with galactic plane and most powerful known source locations, giving the estimate of being located as they are by chance. A conclusion section summarize our arguments and derive first estimate on UHE fluxes.

## 2. Remarks on the role in Lepton and Quark model

The century ended with the final success of the Democrito atomist view of Nature. Indeed at the present we believe that atoms, the "undivisible" constitute of matter, are themselves made up by inner new fundamental "atoms", the elementary fermions known, by their different interactions, under the name of leptons and quarks. We are not yet sure if these particles are themselves really the naked elementary core of matter. Nevertheless everything we see and touch are formed by these lightest and therefore most stable charged leptons

and quarks: the well known lightest charged lepton is the common electron, of unitary electric charge, and the two lightest quarks are the up  $u$  and down  $d$  of fractional respectively charges  $2/3 e$ ,  $-1/3 e$ . Actually, hot dark matter may imply that what we do not see in the galaxy and in the Universe, are made mainly of the lightest stable neutral leptons ( $e^-$ ;  $\nu_e$ ) or more exotic supersymmetric partners.

These two quarks are strongly bounded among them selves in doublets or triplets, by inner strong charges described by SU (3) QCD (or by its gauge boson exchange, the eight spin-one gluons), building up hadrons whose most stable ones are the nucleons: common protons and neutrons.

Nucleons themselves are often bounded together by more complex QCD (or nuclear forces) leading to the "Democratically atomic nucleous". Electrons in atoms are far away from nuclei bounded by the exchange of massless QED gauge bosons, the Einstein (virtual) photons. Lepton number and Quark number conservation is a yet unexplained conservation law, possibly related untested unified gauge theories. Photons themselves, within the unified electroweak  $U(1) \times SU(2) \times$  Weinberg - Salam - Glashow model, share their own identity with heavier gauge bosons: a twin charged pair  $W^+; W^-$  and a heavy neutral photon, the  $Z$  boson, linking and converting leptons to quarks and explaining at once both the Maxwell electromagnetic "lights" and the observed nuclear radioactivity.

The up-down twin quarks, therefore, should be linked to their twin lepton pair. As Pauli and Fermi suggested, by energy conservation arguments, neutrino  $\nu_e$  should exist and it should pair to electron, forming a first complete electron family. Electron neutrino should be extremely light ( $m_\nu < 100$  eV) by the yet undeciphered Yukawa (masses) coupling matrix. Moreover lepton families, as discovered by the earliest astrophysical cosmic ray data (Conversi, Rossi) in 50's, are mirrored in a second heavier and unstable lepton family made by muon and its own corresponding neutrino  $\nu_\mu$ . Finally in 70's a third heavier lepton family arose: the tau and its complementary partner  $\nu_\tau$ . The last neutrino, while being necessary, it has not been yet directly observed. This is mainly due to its fast decay. Because of parity, charge, and symmetries (PCT) these six leptons and their

six quarks associated have their own antiparticle leading to full antimatter counter partner.

The corresponding third quark family, the heavy top, has been only recently (1994) detected experimentally, leaving only the and as the unique fundamental lepton quark unobserved today.

The lepton and quark are commonly described in the following scheme:

$e^-$		
$e^-$		
$u$	$c$	$t$
$d$	$s$	$b$

Following Cabibbo (1964) flavor mixing for quarks, B. Pontecorvo (1967) promptly suggested a neutral lepton mass mixing responsible of light neutrino flavor changing. The obvious need of a non vanishing neutrino mass led to a wide chain of consequences in astrophysical and cosmological problems, ranging from dark matter role (Hot Dark Matter) in closure of the Universe, galaxy formation and dark halos. Therefore the (probable) heaviest neutral lepton neutrino tau,  $\nu_\tau$ , may deeply influence by its mass the same cosmological past history and future evolution. In particular its early gravitational clustering in galactic halo may offer a very efficient gravitational seed for baryonic clustering (Zeldovich et al. 1980, Fargion 1983), moreover, light while forming dense dark galactic halos, may offer an ideal calorimeter to UHE at GZK energies, solving the UHECR puzzle (Fargion, Male, Salis 1997 - 1999).

The possible presence of an additional fourth neutrino (and quark) family, while unnecessary, it is allowed near  $M_z = 2$  mass and it may lead to very exciting astroparticle consequence and observational possibilities in underground detectors (DAMA) and galactic GeV EGRET diused halo (Fargion, Konoplich, Khlopov, Mignani 1995; Fargion, et al. 1998 - 1999; Fargion, Konoplich, Rossi, Khlopov 2000)

### 3. The neutrino mass in high energy astrophysics and cosmology

Elementary particles, gravity and astrophysics are well linked together (Weinberg 1972, Dolkov Zeldovich 1981). In particular the neutrino mass has a direct impacts in fundamental modern ques-

tions in modern astrophysics:

the solar neutrino puzzle, the supernova neutrino fluxes, the atmospheric neutrino asymmetry, the hot dark matter in galaxy or in galactic cluster halos, the same galaxy formation the cosmological critical mass. Because of the observed mass hierarchy in the lepton sector, neutrino tau may be the heaviest and therefore the dominant one. Moreover neutrino mass may be either of Majorana or Dirac nature, leading to different elementary particle behaviours and early nucleosynthesis evolution (Fargion, Shepkin 1984). The same neutrino mass imply the presence (by Lorentz boost) of the "sterile" right handed partner, whose role may be important in early Universe (Fargion 1981; Antonelli, Konoplich, Fargion 1981) and in highest energy astrophysics. The different  $L_R$  interaction and the different thermal evolutions may lead to different thermal neutrino populations. The multi-dimensional clustering of such massive neutrinos has been widely studied (Zeldovich 1980 et al; Fargion 1983).

Just to emphasize the mass roles respect to massless gravitons, we remind the important case of a SN MeVs neutrino burst arriving slowed by its mass relativistic light and its delayed arrival from far SN (galactic or better extragalactic) events respect to the massless gravitational waves. The expected time delay between the massless graviton wave burst (by supernova quadrupole emission at distance  $L$ ) and the  $e$  neutronization neutrino burst, will be an additional test to the elusive mass detection:  $t = 50 \text{ sec} \frac{E^2}{5 \text{ MeV}} \frac{m^2}{5 \text{ eV}} \frac{L}{M \text{ pc}}$ . (Fargion 1981).

#### 4. The key role of UHE $\nu$ ; and $e$ in $\text{km}^3$ detector

##### 4.1. The UHE $\nu$ ; oscillation length

High energy astrophysics is waiting for the new neutrino telescope generations able to reveal the expected TeV (and above) energetic neutrinos ejected by active nuclei (AGN) blazars as well as from galactic supernova relics or galactic mini-blazars. The common theoretical argument in favor for neutrino cosmic ray (c.r.) source is the last experimental evidence of extra galactic TeV photon sources (Markarian 421, 501) and the unique neutrino transparency through cosmic 2.75 K B.R. from cosmic distances. Secondary

atmospheric neutrinos will play a negligible role at high ( $10^4$   $10^6$  GeV) c.r. energy. The common expected UHE neutrinos are of electronic ( $e$ ;  $\nu$ ) and muonic ( $\mu$ ;  $\bar{\nu}$ ) nature because of the "low energetic" pion progenitor masses ( $m_\pi$ ), and their consequent easier and larger productions in proton-proton scattering. However, at very high energy ( $E_p > 10^{15}$  eV) the p-p scattering may lead, by charm production, to other secondary charmed hadrons able to decay also in tau leptons; this possibility allows (at least above  $10^{15}$  eV) the production of a small component nearly as abundant as  $e$ ; ones. Moreover, flavor mixing and oscillation like ( $\nu_s$ ), even at most wide and unexplored parameter ranges ( $1 > \sin^2 2\theta > 0$ ;  $m_{ij}^2 < 0.2 \text{ eV}^2$ ) are well compatible with characteristic large galactic and huge cosmological lengths  $L_g = 10^4 \text{ cm}$ ;  $L_c = \frac{c}{H_0} = 10^{28} \text{ cm}$ . Indeed the flavor oscillation length is as in eq.1.

$$L_{ij} = (i! j!)^{-1/2} \quad (2)$$

$$1.23 \cdot 10^{16} \text{ cm} \cdot \frac{E}{10^{20} \text{ eV}} \cdot \frac{m_{ij}}{\text{eV}}^2 \cdot L_g \cdot L_c$$

Therefore flavor mixing strongly implied by recent Super-Kamiokande data may easily lead to an abundant production. It should be obvious that there is not room for such an oscillation distance for UHE atmospheric at tens TeV or above in Earth (if  $m_{ij} < 10^4 \text{ eV}^2$ ). However, ultra high energy interactions with matter, deeply overview and summarized by the last reports (Gandhi et al 1996; Gandhi et al 1998), received little attention to the role (probably because of the very short unstable lifetime of the lepton: ( $\frac{m}{m_\pi} \approx 3 \cdot 10^3 \text{ sec}$ ) and its consequent short range track. Nevertheless, a first important UHE role at PeV energies has been noted also recently by (Learned, Pakvasa 1995); in particular, these authors stressed that a characteristic hadronic showering behaviour at the initial event of the  $N$  interaction and at the end of the lepton track: a "double bang" signal.

Here (Fargion 1997a) we underline the dominant and key role of  $\nu$ ; tracks signatures by their secondary tau at much higher energies ( $E > (10^7 - 10^8) \text{ eV}$ ) over muon ones be-

cause of the large Lorentz factors and the consequent longer tau tracks. This relativistic tau "longevity" makes the heaviest lepton the most easily detectable above  $5 \times 10^6$  eV (or  $10^{17}$  eV in the rock) in a  $\text{Km}^3$  detector.

#### 4.2. The tau radiation length versus the muon one

Muons are commonly known as the most penetrating charged cosmic ray because their radiation length is much longer (at high energy) than the corresponding electron one. Indeed, the muon radiation length at high energy is roughly  $\frac{m_L}{m_e}^2$  longer than that of the electron, because (Jackson 1962), eq. 15.48) the characteristic leptonic bremsstrahlung radiation length  $b_L^{-1}$  is found classically:

$$b_L^{-1} = \frac{16}{3} Z^2 N \frac{e^2}{\gamma c} \frac{e^2}{m_L c^2}^2 \ln \frac{192 m_L}{Z^{1/3} m_e} \quad (3)$$

where  $N$  is the atomic number density which is proportional to the Avogadro number times the average density,  $\gamma$  is an dimensional factor near unity,  $m_L$  is the lepton ( $e^-$ ;  $\tau^-$ ) mass and  $Z$  is the target nuclear charge. Therefore neglecting the "slow" logarithmic mass dependence, the radiation length  $b_L^{-1}$  is mainly proportional to the square of the lepton mass  $m_L$ . The radiation loss by pair production would be, at higher energies, the ruling one (over bremsstrahlung and over the negligible photo nuclear losses). Nevertheless, all the radiation lengths grow in similar form i.e., as the square of the lepton mass ( $m_L^2$ ). The reason of it is in the probability amplitude of the corresponding Feynman diagram, where an exchange of a virtual photon by a nuclei and by the incoming relativistic lepton leads to the emission of a high energy photon, or an electron pair. The process amplitude is roughly proportional (because of the lepton mass presence in the propagator) to the inverse of the lepton mass ( $m_L$ ). The consequent cross section and its inverse (roughly proportional to the radiation length) decrease (or grow) consequently as  $\frac{m_L}{m_e}^2$  (or  $\frac{m_L}{m_e}^2$ ) as it has been found classically and experimentally in Eq. 3. Therefore the most penetrating lepton must be the heaviest ones, i.e. the tau leptons. On the

other hand, the lifetime of the unstable tau lepton, being proportional to the inverse of the fifth power of its mass  $\tau \sim \frac{m}{m_L}^5$ , makes its track extremely short:  $c \tau = 9 \times 10^6$  cm (with respect to the muon ones). At higher and higher energies ( $E = 100$  TeV) the huge Lorentz factor boost the observed short tau lifetime and increase its value linearly with energy while the corresponding muon tracks already reached, in the water or in the rock, a nearly steady maximum (a logarithmic growth) of a few kilometers length. Consequently, at highest energy ( $E = 5.6 \times 10^6$  eV in water,  $1.6 \times 10^6$  eV in the rock) the tau radiation length will be the longest one and the cosmic tau neutrino rays, ; (if abundant as other avors) will be the dominant source of signals in  $\text{Km}^3$  detectors over other leptons at the same energies. Naturally, as for the muons as showed in Fig. 1, also the tau radiation length will be slowed down at the highest energies ( $4 \times 10^6$  eV) for two main energy losses:

- a) The electromagnetic radiation losses (pair production). See interaction length  $R_R$  in Fig. 1.
- b) The electroweak interactions and losses with matter (mainly nucleons). See interaction length  $R_W$  in Fig. 1.

The latter processes is the main restrictive constraint on tau tracks (in water and rock) at  $E = 5 \times 10^6$  eV and it provides a maximum radiation length comparable to those of the neutrino at same energies ( $220 \text{ km}$  in the rock,  $498 \text{ km}$  in water) which will be discussed further in detail, below. The growth of the lepton radiation length and its (proportional) detectability leads to a fundamental and dominant role of UHE ( $10^6$  GeV) astrophysics, in a near future  $\text{Km}^3$  or larger neutrino telescope. Contrary to present arguments, we remind that the absence of fluxes when flavour oscillations are forbidden, at lower energies ( $10^{11} - 10^{13}$  eV) has already been considered by us (Fargion et al. 1996), in order to bound the annihilations properties of any hypothetical heavy fourth neutrino generation clustered, as cold dark matter, in galactic halos.

The large ratio of the radiation length over those of the muons, reaching in principle a maximal factor  $\frac{m_L}{m_e}^2$  (or at least two order of

magnitude), might imply a corresponding ratio in the detectability of the two leptons at those energies ( $10^8 - 10^9$  GeV); however nuclear interactions mentioned above and as shown later make this ratio smaller (< 20).

Finally, the secondary muons 'tail' due to decays ( ) will also increase by a large fraction (> 100%) the indirect (and ) detectability. Moreover, the most probable (> 60%) hadronic decay (and its consequent shower) or its electroweak nuclear shower will lead as it has been noted (Learned & Pakvasa 1995) to an unambiguous 'hadronic' jet signature in underground detectors, contrary to common 'quite' one-track muon leptonic decays. Finally as suggested in section 7 the decay of ultra high energy secondaries born by  $\pi^+$  inside a mountain and emerging in a deep valley or in upward air shower may lead to detectable signals.

## 5. The source of high energy ;

Ultra-high energy neutrinos ( $e^-; \bar{e}$ ;  $\nu$ ;  $\bar{\nu}$ ) ( $E > 10^{19}$  eV) may be born either by nucleons events in Quasars or blazars cores, or copiously by photopion production of high energy proton (and neutron) ( $E_p > 10^{19}$  eV) onto cosmic 2.75K BBR and galactic radio waves background (the GZK cut-off). Unfortunately, these abundant photopion productions at  $10^8 - 10^9$  GeV cannot in general produce direct tau neutrinos. Nevertheless, there are other reactions able to lead to primary or secondary high energy tau and :

- a) charged neutrino-electron interactions; ( $e^- e^-$  !) at the resonance  $W^-$  mass peak relevant only at energy peak  $E = 6 \text{ GeV}$ .
- b) Flavor oscillations ! following last evidences by SuperKamiokande, at the widest and even unexamined parameter ranges: ( $1 > \sin^2 2\theta > 0$ ), ( $1 > \sin^2 2\delta > 0$ );  $m_{\nu_3}^2 = 0.002 \text{ eV}^2$  (1). For any realistic neutrino mass these parameters may be satisfied. Indeed, flavor oscillation lengths, as already mentioned, even stretched by the huge Lorentz factor is in general below to characteristic cosmological  $\frac{c}{H_0}$  distances: (see Eq. 2).
- c) Topological defects may inject directly abundant UHE : this cosmological relics may

pollute cosmic rays above GZK constrains (Sigl et al 1998). However recent proposal (Fargion et al 1997; Fargion et al 1999) to overcome GZK puzzle, based on UHE neutrino interactions onto relic light ones in clustered galactic halo (Fargion et al 1999), also imply a higher primary and secondary neutrino flux (Yoshida et al 1998).

Finally we remind that ultra high energy tau pairs production, by high energy photon ( $E = 5 \text{ TeV}$ )-photon (BBR at 2.7 K) Compton Scattering, may also take place, but at a very low rate with respect to pion productions. Therefore we shall consider in the following the neutrino and anti neutrino tau cosmic ray fluxes as abundant (or comparable) as all the other avors ones. Astrophysical sources and fluxes for such a high energy ( $10^7 - 10^9$  GeV) neutrinos have been modeled by many; we refer mainly to the flux calculated by (Stecker et al 1991) which will probably dominate in the energy range ( $10^6 - 3 \text{ GeV}$ ), labeled by AGN-SS91 (Gandhi et al 1996, in Fig. 18) and also (Gandhi et al 1998, in Fig. 9) (Fig. 2) due to p-p scattering at source; in this range and scenario we must expect primary . We also refer to the photopion production of cosmic rays and the secondary neutrino flux ( $e^-; \bar{e}; \nu; \bar{\nu}$ ) considered by (Yoshida & Teshima 1993) either for turn-on QSRs time at maximal redshift  $z = 2$  (labeled by CR{2 in (Gandhi et al 1996)) and redshift  $z = 4$  (labeled by CR{4 in (Gandhi et al 1996)) and models by M anneheim AGN-M 95 et Protheore AGN-P 96 (Gandhi et al 1998) (Fig. 2). For the last two models the expected neutrino maximum fluxes at the neutrino energy range  $3 - 5 \text{ GeV}$  reaches a value  $10^{17} \text{ cm}^{-2} 10^{18} \text{ cm}^{-2} \text{ s}^{-1} \text{ sr}^{-1} 10^{17} \text{ cm}^{-2} \text{ s}^{-1} \text{ sr}^{-1}$  i.e. fluxes one or two order of magnitude above to those observed at the same energies in known cosmic rays on Earth; these fluxes are comparable to the ones needed to explain the UHECR puzzle above the GZK cut-off by neutrino-neutrino interactions in galactic halo (Fargion et al 1997; Fargion et al 1999). The overall fluence spectra ( $\frac{dN}{dE}$ ) of UHE models, following (Gandhi et al 1996) is summarized in g.2.

## 6. Interaction ranges of ultra high energy tau lepton

As we already mentioned the radiation length  $b^1$  for tau lepton, due mainly to pair production in Eq. 3, will increase the range of tau tracks (energy dependent) with respect to corresponding of muons, as soon as the Lorentz boost ( ) will reach large values ( $> 10^8$ ) and as long as the electro weak interaction with nucleons will not bind their growth.

The radiation length  $b^1$  will play a role in defining the tau range by the general energy loss equation:

$$\frac{dE}{dx} = a(E) + b(E)E ; \quad (4)$$

where  $a$  and  $b$  are slow energy variable functions respectively for ionization and radiation losses. The asymptotic radiation length  $b^1$  at high energies  $E = 10^{15}$  eV is related to the corresponding muon one by this approximated relation derived by classical bremsstrahlung formula in Eq. 3 scaled for the two different lepton masses:

$$b' = \frac{m_e}{m_\tau}^2 \frac{2}{4} \frac{\ln \frac{192m_e}{z^{1/3}m_\tau}}{\ln \frac{192m_\tau}{z^{1/3}m_e}}^3 b = \quad (5)$$

$$= \frac{b}{219} = 1.78 \cdot 10^8 \text{ cm}^{-1} r^{-1} ;$$

where,  $r^{-1}$  stand for relative adimensional density in water unity, and where in the present energy range,  $E = 10^5$  eV, we assumed that the experimental phenomenological coefficient as in (Gandhi et al 1996):  $b' = 3.9 \cdot 10^8 \text{ cm}^{-1} r^{-1}$ . The corresponding radiation length  $b^1$  is:  $b^1 = 561 \text{ Km}$ . The ionization coefficients values are:  $a' = 2 \cdot 10^8 \text{ cm}^{-1} \text{ eV}^{-1}$ . The integral of the energy loss equation will lead, from the radiation length  $b^1$ , to a larger, energy dependent, radiation range  $R_R$ :

$$R_R = \frac{b^1}{r} \ln \frac{a + bE}{a + bE^{\text{min}}} , \quad \frac{b^1}{r} \ln \frac{E}{E^{\text{min}}} \quad (6)$$

The last approximation occurs because of the smallness (for  $E = 10^5$  eV) of the ionization factor  $a$  with respect to  $bE^{\text{min}}$  and  $bE$  term s.

In the Earth, according to the preliminary Earth Model (Gandhi et al 1996, 1998) on the first few Km the relative density  $r$  is unity in the sea, near 3 in the early depth rocks, around 5 in the first 1000 Km Earth depths. Therefore the consequent tau radiation length from Eqs. 5-6 (for  $r = 5$ ),  $E = 10^4$  eV becomes:

$$R_R = 1033 \text{ Km} \cdot \frac{r}{5}^1 \quad (7)$$

$$\frac{8}{\approx} \frac{\ln \frac{E}{10^8 \text{ eV}}}{1 + \frac{\ln \frac{E^{\text{min}}}{10^4 \text{ eV}}}{(\ln 10^4)}}^9 \approx \dots$$

This extreme propagation range, comparable even to the Earth radius, is to be combined with and bounded by, the more restrictive tau lengths due to short tau lifetime, as well as by the range due to electro weak tau-nucleons interactions at the highest energies ( $E = 10^8$  eV).

The role of tau lifetime and its free path length  $R_\circ$ , boosted by large Lorentz factors  $\gamma = \frac{E}{m_e c^2}$ , grows linearly with energies:

$$R_\circ = c = 5 \text{ Km} \cdot \frac{E}{10^8 \text{ eV}} : \quad (8)$$

The electro weak tau-nucleon interaction range,  $R_W$ , on the other side, decreases with tau energies in analogy with the corresponding ones for neutrino-nucleon scattering (following parton model). In a first approximation the cross sections ( $\langle N \rangle$ ), at energy of interest  $10^6$  eV  $E = 10^{12}$  eV may be described by a simple power law form, either for charged and neutral currents; because of the crossing symmetry in the Feynman diagram we may also write (following updated (Gandhi et al 1998)) similar expressions for ( $\langle N \rangle$ ):

$$\begin{aligned} \text{cc}(\langle N \rangle) &= 4.43 \cdot 10^{33} \text{ cm}^2 \cdot \frac{E}{10^8 \text{ eV}}^{0.363} \\ \text{nc}(\langle N \rangle) &= 1.35 \cdot 10^{33} \text{ cm}^2 \cdot \frac{E}{10^8 \text{ eV}}^{0.363} \\ \text{cc}(\langle N \rangle) &= 4.42 \cdot 10^{33} \text{ cm}^2 \cdot \frac{E}{10^8 \text{ eV}}^{0.363} \\ \text{nc}(\langle N \rangle) &= 1.84 \cdot 10^{33} \text{ cm}^2 \cdot \frac{E}{10^8 \text{ eV}}^{0.363} \end{aligned} \quad (9)$$

The corresponding averaged electroweak range  $R_W$  in the energy range of interest in water for a total (charged + neutral) cross sections ( $N$ )'  $(N)' 6.3 \cdot 10^3 \text{ cm}^2 \frac{E}{10^8 \text{ GeV}}^{0.363}$  is:

$$R_W = \frac{1}{N_A r}, \frac{2.6 \cdot 10^3 \text{ m}}{r} \frac{E}{10^8 \text{ GeV}}^{0.363} : \quad (10)$$

The total tau range,  $R$ , is just the minimal value of the three above ones: the radiation one  $R_R$  in Eq. 6, the lifetime one  $R_\tau$  in Eq. 8, the present electroweak-nuclear one  $R_W$  in Eq. 10:

$$R = \frac{1}{R_R} + \frac{1}{R_\tau} + \frac{1}{R_W} \quad : \quad (11)$$

Let us notice that in the estimate of the electroweak range  $R_W$  we neglected the (otherwise) interesting electron-tau electroweak interactions in the atoms for two main reasons:

- a) The tau-electron electroweak cross sections ( $e^- \tau^- e^-$ ) do not experience the (corresponding) resonant peak (as for neutrino-electron scattering:  $e^- \bar{W}^- \tau^- e^-$ ) at energies  $E > 6 \cdot 10^8 \text{ GeV}$ . The analogous resonant reaction ( $e^+ \tau^+ Z_0^- \tau^- e^-$ ) is forbidden by flavor conservation number. Tau and electrons may only interact weakly by electroweak exchange of a neutral virtual boson  $Z_0$  and a photon.
- b) Even in the above (not allowed) case of a resonant cross section at energy  $E > 6 \cdot 10^{15} \text{ eV}$  and cross section  $\sigma_e > 10^{31} \text{ cm}^2$ , the shortest tau lifetime and its range  $R_\tau$ , in Eq. 11, will mask and hide the short range  $R_W$  (due to hypothetical e "resonant" scattering).

It is important to consider the tau range  $R$  at its characteristic regimes: when its value will overcome the corresponding muon one  $R$  ( $R = R_\tau$ ), when it will reach its maximal extension  $R = R_{\max}$ , when it will be confined (because of nuclear interactions) at the highest energies to the same ranges as muon tracks ( $R = R_W = R$ ).

## 6.1. The critical energies for dominance

Let us define the first critical energy,  $E_1$ , where the tau range equals the muon one:  $R_\tau = R$  from (Eq. 11), (Eq. 6) and (Eq. 3) by substitution of  $b$  with  $b_\tau$ . This equation may be easily solved noticing that at this energy range ( $E = 10^8 \text{ GeV}$ ) the shortest and main tau range is the lifetime one,  $R_\tau = R$ ; therefore the equation  $R_\tau = R$  can be written as follows:

$$R_\tau = R = c \frac{E}{m c^2} = \frac{1}{b_\tau r} \ln \frac{a + b E}{a + b E^{\text{min}}} \quad (12)$$

where one imposes  $E = E_1$ ; numerically one finds that

$$5 \text{ K m} \frac{E}{10^8 \text{ GeV}} = \frac{2.65}{r} \ln \frac{E}{E^{\text{min}}} \text{ K m} \quad (13)$$

defines the critical energy  $E_1$  where tau track exceeds the muonic one. For water  $r = 1$ , and rock (in these depths  $h_{\text{rock}} = 3$ ) the critical energy  $E_1$  and the tau range  $R_1$  are:

$$E_1 = 5.6 \cdot 10^8 \text{ GeV}; \quad E_1 = 1.65 \cdot 10^8 \text{ GeV} \\ (\text{water}) \quad (\text{rock})$$

$$R_1 = 28 \text{ K m}; \quad R_1 = 8.2 \text{ K m} \quad (14)$$

Here we considered  $E^{\text{min}} = 10^4 \text{ GeV}$  as in (Gandhi et al. 1996). Let us remind that the analytical curve we are using in Eq. 6 for muons is a bit overestimated with respect to a more detailed study (Lipari and Stanev 1991) and therefore the present critical "analytical" value  $E_1$  and the range  $R_1$ , might be larger than the real one (by a factor 1.5–2). Therefore from energies  $E > 10^8 \text{ GeV}$  above the tau signal will overcome the muon ones. Moreover, the prompt secondary muons from tau decays or from tau hadronic pions decays (let us label them  $\tau'$ ), may in principle "double" the expected muonic fluxes; finally the characteristic tau hadronic decay ("Learned & Pakvasa 1995, "bang") may leave

a unique signal, as we shall see, in upward air shower.

The linear growth of the range  $R$ , in absence of the  $N$  weak interactions, would reach a maximal radiation range  $R_R$  (due to maximal  $b^1$  in Eq. 5) as in Eq. 7, at least two orders of magnitude larger than the corresponding muon range ( $R$ ). Indeed, it is possible to show that in such an ideal (no-electroweak interactions) case the relation  $R_\tau = R_R$  would define an extreme energy  $E_\tau \approx 4 \cdot 10^6$  GeV and a corresponding range  $R_\tau \approx 2000$  Km, much longer than the  $R_R$  range (at the same energy in the rock):  $R_\tau (4 \cdot 10^6$  GeV) = 14 Km.

However, the maximal tau range is bounded by the more restrictive electroweak cross sections (in Eq. 9) (as for neutrinos) and its range  $R_W$  (in Eq. 10). The maximal tau range  $R_{\max}$  is then defined by equal conditions in Eqs. 8 and 10, ( $R_\tau = R_W$ ):

$$R_\tau = 5 \text{ Km} \quad \frac{E}{10^8 \text{ GeV}} = \quad (15)$$

$$= \frac{2.65}{r} \cdot 10^6 \text{ Km} \quad \frac{E}{10^8 \text{ GeV}}^{0.363} ;$$

whose solution is (for  $r = 3$  as in the few hundred terrestrial Km depths):

$$R_{\max} = 223 \text{ Km} \quad \frac{r}{3}^{\frac{1}{0.363}} \quad (16)$$

$$E_{\max} = 4.45 \cdot 10^6 \text{ GeV} \quad \frac{r}{3}^{\frac{1}{0.363}} :$$

For the peculiar case ("horizontal" neutrinos arrivals), in the sea, where we may assume  $r = 1$ , at a detector depth 10 Km, and a sea 20 Km depth, one gets  $R_{\max} = 498$  Km;  $E_{\max} = 9.97 \cdot 10^6$  GeV.

It is clear that from the Equation above the total maximal tau range  $R_{\max}$  extends above 20 times the corresponding muon range at the same energies. This imply a 20 fold more penetrating horizontal traces in Km<sup>3</sup> detectors. If we could observe the complete lepton horizontal tracks up to L Km we would count, for L = 500 Km, an extreme ratio  $N = N_e^{20} \approx 2 \cdot 10^6$ .

Finally at higher energies also the electroweak interaction will bound the muon radiation range and it will make comparable both the tau's and muon's ranges. This will occur once the relation  $R_\tau / R_W = R$  at the same energy  $E_\tau = E$  (in Eqs. 3(6) and Eq. 10) is satisfied; i.e. when

$$R_\tau = \frac{b^1}{r} \ln \frac{E}{E_{\min}} = R_W = \frac{1}{w N_A r} : \quad (17)$$

This relation implies, for an adimensional density  $r = 3$  a critical energy and ranges:

$$E_\tau \approx 1.7 \cdot 10^6 \text{ GeV} ; R_\tau / R_W = R = 16 \text{ Km} : \quad (18)$$

## 6.2. The UHE observability in underground detectors

Therefore from energy  $E_1 = 1.6 \cdot 10^6$  GeV up to the energy  $E_2 \approx 1.7 \cdot 10^6$  GeV, the tau tracks will overcome the muon lengths and it will imply a dominant role for tau neutrino astrophysics (assuming, of course, a corresponding  $e$ ; spectra). This dominance may be detectable in horizontal rates in future underground Km<sup>3</sup> detectors (either of water or ice). The exact signature, of course, depends on the unknown primordial cosmic flux: assuming, as in (Gandhi et al. 1996) or more recent review and models as shown in (Gandhi et al. 1998) a model flux labeled CR{2 and CR{4, whose event rates are summarized in Table 6 (Gandhi et al. 1996), the consequent tau event rate may be promptly derived by scaling the  $R$  range in place of  $R$  for effective Km<sup>3</sup> volume made by the effective area  $A : A_{\text{HR}}$ . The most optimistic rates for downward neutrinos (parton distribution, a CR{4 model, in (Gandhi et al. 1996)) above  $10^7$  GeV may reach a muon event rate a year of  $4.8 \cdot 10^{-2}$  and a corresponding rate increased just near the unity for the longest tracks at its maximal range extension  $R_{\max}$  in Eq. 16. Therefore the  $10^8 - 10^9$  GeV energy window dominance is at present models just at the edge of detectability at near future Km<sup>3</sup> detectors. However, more yet unobserved and abundant ultra high neutrinos fluxes, may increase drastically our predictions. The and presence may also be discovered by other indi-

rect effects: as described in next section, by air shower.

### 6.3. The resonant $e^+e^-$ events in $Km^3$ detectors: the hidden signature of tracks

It is worth to mention that the important and detectable tau contribution in downward  $e^+e^-$  events at energy tuned at the resonant  $W$  formation mass in  $e^+e^-$  collisions:  $E^{\text{res}} = \frac{M^2_W}{2m_e} = 6.3 \cdot 10^6 \text{ eV}$ ; at these ranges of energies the muon range is a few  $Km$  s long while the tau range  $R_\tau \approx R_\mu$  due to an average secondary energy  $hE_\tau \approx \frac{1}{4}E = 1.4 \cdot 10^6 \text{ eV}$  is only  $R_\tau \approx 71 \text{ m}$ . Therefore PeV tau ranges are nearly two orders of magnitude smaller than those of the muons.

The expected downward muon number of events  $N_{\text{ev}} (e^+e^-)$  in this resonant energy range, in  $Km^3$ , (Gandhi et al. 1998, Table 7) was found to be  $N_{\text{ev}} = 6$  a year. One expects (Gandhi et al. 1998) a comparable number of reactions ( $e^+e^-$ ). However the possible presence of primordial  $\nu$ ; by flavor mixing and  $\nu N$  charged current interactions lead to a factor 5 larger rate,  $N_{\text{ev}} = 29$  event/year.

Moreover assuming ultra high energy cosmic primary rays at energy range  $10^7 \text{ GeV} > E > 10^4 \text{ GeV}$ , the same nuclear electroweak  $N$  interactions, (which lead to (and) opacity through the Earth at highest energies), are a source of copious horizontal secondaries (even in the energy range where the tau tracks are not longer than the muon ones). Indeed, in the energy range  $10^5 \text{ GeV} > E > 10^4 \text{ GeV}$  the tau production (by  $eN \rightarrow e^+e^- + \text{anything}$ ) is almost identical to the muon one. The only difference is due to the range length of tau  $R_\tau \approx 50 \text{ m} \approx \frac{E}{10^6 \text{ GeV}}$  to be compared with a few kilometer of a muon radiation range (very sensitive to the exact  $E$  in cut-off).

Only 18% (of these 20% of events) will mask their tau nature by a  $e^+e^-$  decay, nearly at the same energy direction and therefore hidden in a unique muonic track. Most (82%) of the above events will mark their identity by a  $50 \text{ m} \approx \frac{E}{10^6 \text{ GeV}}$  tau precursor track either with a spectacular and characteristic tau-hadronic shower (a jet) (64%) and by a short and intense electron shower (whose length, by Landau, Pomoranchuk & Migdalek (2), is as short as  $R_e = 4 \text{ m} \approx \frac{E}{6 \cdot 10^5 \text{ eV}}^{1/2}$ ) or, as

noted in (Learned & Pakvasa 1995) by their double "bangs". From the arguments above we nearly expect 35 downward events a year to be associated with precursor tracks; other 10 (upward)

PeV events may bring the imprint (and direction) of primary cosmic rays born in Active Galactic Nuclear (AGN) or in galactic jets. These expectations may reach hundred events a year for most optimistic and abundant spectra of sources (Gandhi et al. 1996, Fig 2). Because of UHE opacity in Earth above PeVs one should see a marked anisotropy in  $Km^3$  favoring UHE tracks at horizontal arrival plane (5°). How can one better exploit the longevity of UHE near and above PeV?

## 7. UHE detected by air showers

### 7.1. Horizontal air shower beyond a mountain as an UHE amplifier

As we have seen the UHE muon and tau tracks in  $Km^3$  detector above  $Km$  length are difficult to be distinguished: a shower in water might be either a catastrophic bremsstrahlung muon interaction or a tau decay in flight. The hundred  $Km$ s range of UHE at horizons in limited underground ( $Km^3$ ) detector are not distinguished from PeVs. In order to recognize with no ambiguity each lepton nature we propose here and in more detail elsewhere, a new detector able to filter and to reveal tau leptons (Fargion, Aiello, Conversano 1999). We suggest to consider for this aim a deep valley as the Grand Canyon in USA or deep valleys near Inyo-Whitney mountains in Nevada as well as the glacial valley in the Alps. It will be possible to observe UHE neutrinos by their contained horizontal showers in huge air volumes. The deep rock walls play the same role of the target beam dump for UHE neutrinos as well as of filtering atmospheric cosmic rays. Moreover the same kilometers volume sizes act as a filter avoiding random atmospheric muon decay but allowing the UHE tau ones at PeVs band. The same rock may increase the target matter (respect to horizontal shower in air as in Auger experiment) by nearly two order of magnitude. At far depth ( $Km$ ) and at horizontal angles ( $60^\circ - 90^\circ$ ) at energies above  $1000 \text{ TeV}$  the atmospheric muon secondaries (crossing two or more  $Km$ s of rock matter) will be negligible, while a primary neutrino

may interact in the rock leading to secondary leptons: only muon and tau tracks are long enough to emerge often from the mountain wall rock. At Z pole ( $E = 6.3 \text{ PeV}$ ), the UHE secondary muon will decay, in empty space, at  $10^7 \text{ Km}$  distance while the corresponding tau at only 70 meters. Such muons may poorly interact by bremsstrahlung in air beyond  $10^4 \text{ Km}$  distances; therefore PeV muons in air will produce sterile single tracks while the corresponding tau should decay leading to copious air shower originated within ten meters from the mountain walls. These bounded horizontal atmospheric showers originated within the deep valley may be observed either by Cherenkov detectors inside the  $\text{Km}^3$  volumes, or more economically just monitoring above the valley, by atmospheric scintillation traces and its fluorescence signals in the dark nights. Our first estimates for horizontal showers is based on an interaction volume defined for example as follows:

Argentier Alps (Fig. 3) chain length '  $10 \text{ Km}$ ; characteristic height  $1 \text{ Km}$ ;  
UHE - energies  $3 \text{ PeV}$  and its distance before the decay  $150 \text{ m}$ ;  
total interactive volume  $V = 4.5 \text{ Km}^3$  (water equivalent).

The air shower tail may be observed also as a burst.

The air shower volume is therefore observable within a narrow beam ed cone ( $\text{Moliere radius } 80 \text{ m} / \text{distance } 5 \text{ Km}$ ): ( $1^\circ, 2 \cdot 10^5$ ) and it is reduced to an effective volume  $V_{\text{eff}} = 9 \cdot 10^6 \text{ Km}^3$  for each observational detector (Fig. 3b). Each one is comparable to roughly twice a Super Kamiokande detector. We expect, following AGN-SS91 model (Gandhi et al. 1998) a total rate of: (6) ( $e^+e^-$ ) + (29) ( $N$ ) =  $35 \text{ UHE}$  event/year/ $\text{Km}^3$ ; at energies above  $3 \text{ PeV}$  we may expect a total rate of  $N_{\text{ev}} = 158 \text{ event/year}$  in this Argentiere mountains valley (Fig. 3a) and nearly  $3.2 \cdot 10^6 \text{ event/year}$  for each detector. A few hundreds of detectors at a hundred meter distance each other should be located along the valley and their signal/noise would be strong enough. The most abundant air-shower signature, after 5 km air distance atmosphere, corresponding to a  $X_0 = 625 \text{ g cm}^{-2}$  radiation length, would be a copious electromagnetic (and often additional hadronic and muonic) air shower whose hard ( $M \text{ eV}$ ) spectra has a rate  $\text{ux}$  at least &

$3 \cdot 10^6 \text{ cm}^{-2} / \text{sec}$ . A few  $\text{m}^2$  scintillator would observe tens (or hundred) of  $M \text{ eV}$  events in a very narrow burst arrival angle and time in a screened (from upper electromagnetic showers above the edge of the target mountain) (Fig. 4) the burst timing signal will be few microsecond long and its directionality would be easily correlated towards the horizontal mountains (Fig. 3b). Technical details will be discussed elsewhere.

## 7.2. Upward air-shower observable from a mountain

As we have shown the small ux and cross section of UHE call for wider and wider target volume. As OWL experimental proposal has noted, the whole Earth may be the ideal beam dump not only for UHECR born in air but also for the UHE upcoming from Earth and their secondaries decaying in space. The UHE N interactions may generate their parental UHE whose consequent air shower will amplify the signal. The Earth opacity at  $3 \text{ PeV}$  has been evaluated (Gandhi et al. 1998) and corresponds in Stecker Salom on model to 5.2 events/ $\text{Km}^3/\text{year}$  for upward muons. The corresponding event birth rate for UHE, (following Sharada Iyer, M. H. Reno and Ina Sarcevic 1999) within a Stecker Salom on UHE ux model, are nearly twice larger:  $N_{\text{ev}} = 10 \text{ event/Km}^3 \text{ year}$ . In a first approximation it is possible to show that the Earth volume observable from the top of a mountain at height  $h$ , due to UHE at  $3 \text{ PeV}$  crossing from below, is approximately  $V = 5 \cdot 10 \text{ Km}^3 \cdot \frac{h}{\text{Km}} \cdot \frac{E}{3 \text{ PeV}}$ . The upward shower would hit the top of the mountain (Fig. 4). For the same air shower beam ing ( $1^\circ, 2 \cdot 10^5$ ) we derive now an effective volume  $1 \text{ Km}^3$ . Therefore a detector open at  $2^\circ$  angle on a top of a  $2 \text{ Km}$  height mountain may observe nearly an event every two months from below the Earth. The gamma signal above few  $M \text{ eV}$  would be (depending on arrival nadir angle) between  $3 \cdot 10^6 \text{ cm}^{-2} / \text{sec}$  (for small nadir angle) to  $10^5 \text{ cm}^{-2} / \text{sec}$  at far distance at  $3 \text{ PeV}$  energies. Below  $M \text{ eV}$  up to tens  $\text{KeV}$  the signal (secondaries bremsstrahlung hard X photons), may be hundred times larger. However, due to the variable Earth opacity with Nadir angle the highest UHE and event would also arrive easily at the horizon leading to a compensation or even an amplification in the average gamma ux at the horizon edge.

At large nadir angle ( $\theta > 60^\circ$ ) where an average Earth density may be assumed ( $\rho \approx 5$ ) the transmission probability and creation of upward UHE is approximately

$$P(\theta; E) = e^{-\frac{2R_{\text{Earth}} \cos \theta}{R(E)}} (1 - e^{-\frac{R}{R(E)}}) : (19)$$

The corresponding angular integral effective volume observable from a high mountain (or balloon) at height  $h$  (assuming a natural target terrestrial density  $\rho = 3$ ) is:

$$V_{\text{eff}} = 0.3 K m^3 \frac{h}{3} \frac{e^{-\frac{h}{3P_{\text{eV}}}}}{K m} \frac{E}{3P_{\text{eV}}}^{1:363} : (20)$$

Because the upward event from UHE above  $3 \text{ PeV}$  are leading to  $10 \text{ event/Km}^3 \text{ year}$ , we must expect an average effective event rate on a top of a mountain ( $h = 2 \text{ Km}$ ) (Fig. 4):

$$N_{\text{eff}} = 8 \frac{\text{events}}{\text{year}} \frac{h}{3} \frac{e^{-\frac{h}{3P_{\text{eV}}}}}{2 \text{ Km}} \frac{E}{3P_{\text{eV}}}^{1:363} : (21)$$

This rate is quite large and the expected air airshower signal (gamma burst at energies  $> 10 \text{ MeV}$ ) should be  $\sim 10^4 - 10^5 \text{ cm}^2/\text{sec}$ , while the gamma flux at ( $< 10^5 \text{ eV}$ ) or lower energies (from electron pair bremsstrahlung) may be two orders of magnitude larger.

A collection of scintillators, screened from upward UHECR electromagnetic showers, (Fig. 3b), may easily discover this UHE ( $\text{PeV}$ ) flux. Detailed scheme will be shown elsewhere. We notice that the horizontal atmosphere (air) target depth ( $360 \text{ water meter equivalent}$ ) at the UHE peak

$10^9 \text{ eV}$ ,  $R = 500 \text{ Km}$  (Eq. 16) is nearly a thousand times smaller than the corresponding one through the Earth crust depth (from the horizon), leading to a corresponding suppression thousand factor in the  $\sim$  visibility from above (respect to those arriving from below the horizon), (Fig 4). In a sentence the upward nearly horizontal UHE neutrino (at GZK) induced air-shower are three orders of magnitude favored respect to downward ones.

### 7.3. The UHE main air-shower channels

The air-shower morphology would reflect the rich and structured behaviours of decay modes. Indeed let us label the main "elegant" UHE decay channels (hadronic or electromagnetic) and the consequent air-shower imprint, with corresponding probability ratio as shown in the Table 1.

This complex air-shower modes would look to different interaction lengths in air at 1 atm atmosphere ( $\sim 300 \text{ meters}$  for electromagnetic interaction length,  $500 \text{ meters}$  for hadronic interaction length or, more precisely  $800 \text{ meters}$  for tau pions secondaries). The consequent air-shower will reflect these imprint multi-channel modes also in its energy and time arrival structured Terrestrial Gamma Flash.

### 7.4. Ultrahigh energy air shower upward toward satellite: TGF events in BATSE data

The possibility for an upper air shower to reach high altitude and hit a satellite is related to a) UHE N interaction probability within Earth b) UHE track in the rock at the upper crust c) decay in flight distance within atmosphere, d) Radiation length in air and air shower amplification and suppression.

The visible Earth surface from a satellite, like BATSE, at height  $h = 400 \text{ Km}$  and the consequent effective volume for UHE N  $\text{PeV}$ s interaction and air shower beam within  $\sim 2 \times 10^5 \text{ rad}^2$  is: (note  $< > \sim 1:6$  because 70 % of the Earth is covered by seas)

$$V_{\text{eff}} = V_{\text{TOT}} \sim 60 \text{ Km}^3 : (22)$$

The effective volume and the event rate should be reduced, at large nadir angle ( $\theta > 60^\circ$ ) by the atmosphere depth and opacity (for a given  $E$  energy). Therefore the observable volume may be reduced approximately to within  $15 \text{ Km}^3$  values and the expected UHE  $\text{PeV}$  event rate is

$$N_{\text{ev}} = 150 \frac{h}{400} \frac{\text{events}}{\text{year}} (E = 3P_{\text{eV}}) : (23)$$

The present rate of observed TGF at best (low threshold and hard channel trigger set up) is much lower (a factor ten), and it may be possible that tens of  $\text{PeV}$  UHE and are the needed ones to

Table 1  
Tau Air Shower Channels

Decay	Secondaries	Probability	Air-shower
!		17.4%	Unobservable
! e e	e	17.3%	1 Electromagnetic
!		11.8%	1 Hadronic
! 0	; 0 ! 2	25.8%	1 Hadronic, 2 Electromagnetic
! 2 0	; 2 0 ! 4	10.79%	1 Hadronic, 4 Electromagnetic
! 3 0	; 3 0 ! 6	1.23%	1 Hadronic, 6 Electromagnetic
! +	2 ; +	10%	3 Hadronic
! + 0 2	; + ; 0 ! 2	5.18%	3 Hadronic, 2 Electromagnetic

overcome the BATSE sensibility threshold. Therefore a small (factor 3–5) exponential suppression, as in Eq. (21), may reduce the  $N_{ev}$  to the observed TGF rate while it may at once slightly increase their intensities.

The last air shower traces by 3 PeV are mainly hard ( $10^5$  eV or above) bremsstrahlung gamma photons by last air shower electron pairs whose approximated flux number is comparable to

$$N \sim \frac{E}{\langle E \rangle} \sim 10 \quad (24)$$

The atmosphere opacity may reduce the final value at least to  $1/3$ :  $N \sim 10^0$ .

The expected  $X^-$  flux at large 500 Km distances, are diluted even within a beam angle  $\sim 2 \cdot 10^5$ , leading to nearly  $f \sim 10^2$  ph/cm $^2$ . The consequent TGF burst flux is  $f \sim 10^0$  events just comparable with TGF observed ones. The characteristic burst duration is defined by L/c few millisecond in agreement with the observed TGF events.

Its bremsstrahlung spectra is hard, as the observed TGF ones.

The possible air shower time structure may reflect the different eight decay channels (mainly hadronic and/or electromagnetic ones).

The complex interplay between UHE interaction with nuclear matter over imposed on  $e^+e^-$  interactions are shown in (Fig.5). The extremely narrow energy window where  $e^+e^-$  rate is comparable to  $N$  while being transparent to Earth makes upward air shower–TGF connection unrelated to

$e^+e^-$  resonant  $W$  events.

The characteristic interaction regions responsible for most PeV vertical upward air shower is within a narrow dashed band described in (Fig. 5).

Peculiar  $N$  interaction (Fig.6) departing from parton model, would lead to a less restrictive UHE – Earth opacity, and a more abundant vertical TGF event rate at higher energy; the TGF data do not support such a large flux variability and therefore it moderately favors the narrow energy window (PeV – few tens PeV) constrained by parton model (Fig. 5).

Indeed the TGF data, collected by NASA BATSE archive and described in Table 1, are located in celestial map (Fig.7a) with their corresponding error boxes (Fig.7b). They are better readable, after few error bar calibrations, in a galactic map over the di used GeV – EGRET gamma background signal (Fig. 8).

The surprising clustering of TGF in the galactic plane and their correlations with important known TeV,  $\gamma$ ,  $X$  sources, make more plausible the TGF astrophysical nature than any random terrestrial lightning origin (Fig.9). Additional correlations occur with AGASA UHECR (Hayashida et al. 1999) inhomogeneities at EeV energy band (Fig. 10), as well as with most COMPTEL sources as the  $l = 180^\circ$  inhomogeneity.

Some important locations of known galactic and extragalactic source (as nearby QSRs 3C 273 and 3C 279) are listed in Table 2. The 28 absent TGF data may hide, we presume, and predict important evidences of the TGF – air shower connection.

## Conclusions

In this article the UHE , propagation and the UHE air shower role have been analyzed. It has been shown that UHE horizontal and upward air shower within E & 3 PeV may be observable and very probably have been already observed in upward BATSE -TGF events. The distribution of 7 (or 8) TGF events within a sample of 47 events at

<sup>3</sup> along the galactic plane may occur (Fig.11) by chance (Poisson distribution) once over a hundred (or over 500) and it strongly favors the TGF - air shower connection (Fargion, Aiello,2000). Similar conclusion arise from larger angle TGF data clustering from galactic plane ( 10% ) (Fig.12), but do not arise (as it should be expected) for too large angles ( 20° ) from galactic belt (Fig.13). <sup>3</sup>.

Moreover the coincidence in direction (Table1<sub>b</sub>) and in time (Table1<sub>c</sub>) (repeaters) structure of some TGF events (shown by corresponding color mark in Table1<sub>a</sub>) make very probable their characteristic correspondence to active source (blazing galactic and extragalactic sources).

The observation of known source toward Anti Galactic Center (Crab, PKS 0528, Geminga) or toward the Galactic Center (PSR 1706-44, PKS 1622-297, Rho Oph.) or in the Galactic Plane (Cyg X-3, Cyg A, Tycho SNR, COS-B) imply a minimum distance and a consequent lower bound distance (. 4 Kpc) in the oscillation  $\pm$  distance, and a consequent corresponding first upper bound to their square mass mixing:  $m \pm 10^{-8}$  ev<sup>2</sup>.

Therefore the need of UHE call for a very mixing and mass as Superkamiokande atmospheric neutrino imply. A first rough consequence of the few observed event is the existence of a photon opacity both at a galactic and at extragalactic regions at a level comparable to Stecker, Salomon model predictions (1991) , at a rate (one month) (at PeV's energy) (1 - 5)  $10^6$  event/cm<sup>2</sup>/sr. Because of the compelling role UHE N interactions in TGF events we are really testing also the same existence of neutrino. Even it may be possible that all the above correlations occur

by statistical coincidence, we do not believe that Nature would be so perverse in making two completely different signals ( upward air shower and TGF ) by chance. Nevertheless Physics is an Experimental Science. Therefore an additional word should be also found within the 28 missing (secret) TGF data of BATSE experiment. Indeed the GRO BATSE satellite is the most sophisticated and revolutionary detector which opened, in last decade, new golden pages in astronomy. We are curious to know their final response: their data may open and confirm the new exciting UHE neutrino astronomical window .

## Acknowledgments

This work originated at Technion Institute (Fargion 1997). The author thanks Prof A. Dar and M. Bilenky for encouragement, Dr. F. Cesini for important suggestion on statistics, Prof. Barbara Meli, Prof. Tommasina Coville, for useful comments, suggestion and support, Pier Giorgio De Sanctis Lucentini for graphical and computer elaboration. The author is also grateful to Dr. Marco Rossi for warm support and fruitful comments, to Dr. Andrea Aiello for first numerical simulation and to Dr. Roberto Conversano for last reading and correction of the text. This work is based among the others on the Bruno Rossi and Marco Coville discoveries and understanding of cosmic rays and their opening of the lepton and quark physics; in particular this paper is devoted to the memory of Bruno Pontecorvo, father of modern neutrino physics and astrophysics.

<sup>3</sup>A natural question may arise: could the repeated TGF be a brief sequence of lightning? The answer (for all published BATSE data) is definitely no. Because the GRO goes at equator at 8 Km / sec, within a few hundred of second, it will be far from its original geophysical region .

## REFERENCES

S. Weinberg, *Gravitation and Cosmology*, ed. J. Wiley & Sons (1972)

A. Dolgov and Y. Zeldovich, *Rev. Mod. Phys.* 53, 1, (1981)

B. Rossi, *Cosmic Rays*, McGraw-Hill, NY 1964.

Dar, A. & Laor, A. 1996, *astro-ph/9610252*; *ApJ Lett.* (97).

Gandhi, R., Quigg, C., Reno, M. H., Sarcevic, I., 1996, *Astropart. Phys.* Vol 5, 81

J. G. Learned & Pakvasa, S. 1995, *Astropart. Phys.* 3, 267

Jackson, J. D., 1962, *Classical Electrodynamics*, J. Wiley, USA

Fargion, D., Khlopov, M. Yu., Konoplich, R. V., Konoplich, V. K., Mignani, R. 1996, *Modern Phys. Letters A*, 11 (17), 1363-1369

Bilenky, S. M., Pontecorvo, B. 1980, *Phys. Lett.* 95B, 233

Fargion, D. & Shepkin, M. 1984, *Phys. Letters*, 146B, 46 Rubbia, A. 1995, *Nucl. Phys. B (Proc. Suppl.)*, 40, 93

Stecker, F. W., Done, C., Salomon, M. H. & Sommers, P. 1991, *Phys. Rev. Lett.*, 66, 2697

Yoshida, S. & Teshima, M. 1993, *Prog. Theoret. Phys. (Kyoto)*, 89, 833

Landau, L. D. & Ya Pomeranchuk, I., Dokl. Akad. Nauk SSSR, 92, 535; Migndal, A. B. 1956, *Phys. Rev.*, 103, 1811

Gandhi, R., Quigg, C., Reno, M. H., Sarcevic, I., *Phys. Rev. D* 58, 1998; *hep-ph/9807264*.

Fargion, D. Salis, A. Proc. 25th ICRC. HE-4-6, 153-156 (1997).

Fargion, D. M. ele, B. *astro-ph/9902024*; 2nd Dark Matter, Buxton, UK; ed. Spooner, Kudryavtsev; (1999); *astro-ph/9906451*, 26th ICRC Conference, Salt Lake, USA, OG 32.30, Vol 4 p 287 (1999).

Lipari, P. Stanev, T. *Phys. Rev. D* 44 3543 (1991).

Sigl, G., Lee, S., Bhattacharjee, P., Yoshida, S. *hep-ph/9809242*

D. Fargion, *astro-ph/9704205*

D. Fargion, A. Salis, B. M. ele, *Ap. J.* 517 1999; *astro-ph/9710029*.

D. Fargion, *Nuovo Cimento* Vol. 31, No. 49, (1981)

F. Antonelli, R. Konoplich and D. Fargion, *Lett. Nuovo Cimento* Vol. 32, No. 289, (1981)

D. Fargion, *Lett. Nuovo Cimento* Vol. 77B, No. 111, (1983)

D. Fargion, M. Shepkin, *Phys. Letters*, 146 B, 46, (1984)

D. Fargion, M. Khlopov, R. Konoplich, R. Mignani *Phys. Rev. D*, Vol. 52, 1828, (1995)

D. Fargion, M. Khlopov, R. Konoplich, R. Mignani, *Phys. Lett.* 68, 685-690 (1998), D. Fargion, Yu. G. Golubkov, M. Khlopov, R. V. Konoplich, R. Mignani, *Jetp. Lett.* 69, 434-440 (1999); *astro-ph/9903086*.

D. Fargion, A. Aiello, R. Conversano, 26th ICRC Salt Lake, USA, HE 6.1.10, 396-398 (1999); *astro-ph/9906450*.

D. Fargion, R. Konoplich, M. G. Rossi, M. Khlopov, *Astroparticle Physics* 12, 307-314 (2000); *astro-ph/9809260*.

D. Fargion, A. Aiello, (in preparation, 2000)

D. Fargion, M. G. Rossi (in preparation, 2000)

Y. Zeldovich, A. A. Klypin, M. Yu. Khlopov, V. M. Chetchetkin, *Sov. J. Nucl. Phys.* 31 (1980) 664.

Y. N. Hayashida et al. 26th ICRC Salt Lake, USA, HE, (1999); *astro-ph/9906056*.

Fig. 1. The tau ranges as a function of the tau energy respectively for tau lifetime (dashed line)  $R_\tau$ , Eq.8, for tau radiation range  $R_R$ , Eq.7 (short dashed line above) and tau electroweak interaction range  $R_W$ , Eq.10 for two densities  $r$  (long dashed lines, continuous) and their combined range  $R$ , from Eq.11. Below the corresponding radiation range  $R$  for muons (dotted line).

Fig. 2. The Gandhi et al (1996) expected UHE neutrino Neutrino source for different UHE neutrino source models.

Fig. 3a. A panoramic view of The Alps Argentier Mountain chain.

Fig. 3b. A schematic draw of horizontal air shower originated by a mountain chain and the detailed and enlarged scheme of the  $\pi^0$  burst secondaries signal; a shield from downward electromagnetic airshower is described.

Fig. 4. A schematic geometrical draw of the nearly horizontal upcoming air shower cones, both from above and from below the Earth crust, target of UHE neutrino interaction and consequent airshower.

Fig. 5. The Gandhi et al (1998) UHE neutrino ranges as a function of UHE neutrino energy in Earth with overlapping anti neutrino-electron electron and neutrino N interactions; below the UHE range, as in Fig 1, at the same energies in matter (water).

Fig. 6. The Gandhi et al (1998) UHE neutrino ranges as a function of UHE neutrino energy in Earth with overlapping anti neutrino-electron electron and neutrino N interactions; different weaker UHE interaction models are also present.

Fig. 7a. Terrestrial Gamma Flash in celestial coordinate without error bar.

Fig. 7b. Terrestrial Gamma Flash in celestial coordinate with error bar.

Fig. 8. Terrestrial Gamma Flash in celestial coordinate over EGRET GeV di used galactic background.

Fig. 9. Terrestrial Gamma Flash data and relevant known TeV, X, galactic and extragalactic Source in red dots as in Table 2.

Fig. 10a. Terrestrial Gamma Flash in celestial coordinate over UHECR di used data by AGASA cosmic rays at EeV energies.

Fig. 10b. Terrestrial Gamma Flash in celestial coordinate over UHECR di used data by AGASA cosmic rays at EeV energies with relevant known TeV, X, galactic and extragalactic Source in red dots as in Table 2.

Fig. 11. Poisson probability distribution (and simulation) to find by chance  $N = (7=8)$  TGF events within 3 degrees from the galactic plane.

Fig. 12. Poisson probability distribution (and simulation) to find by chance  $N = (14=15)$  TGF events within 10 degrees from the galactic plane.

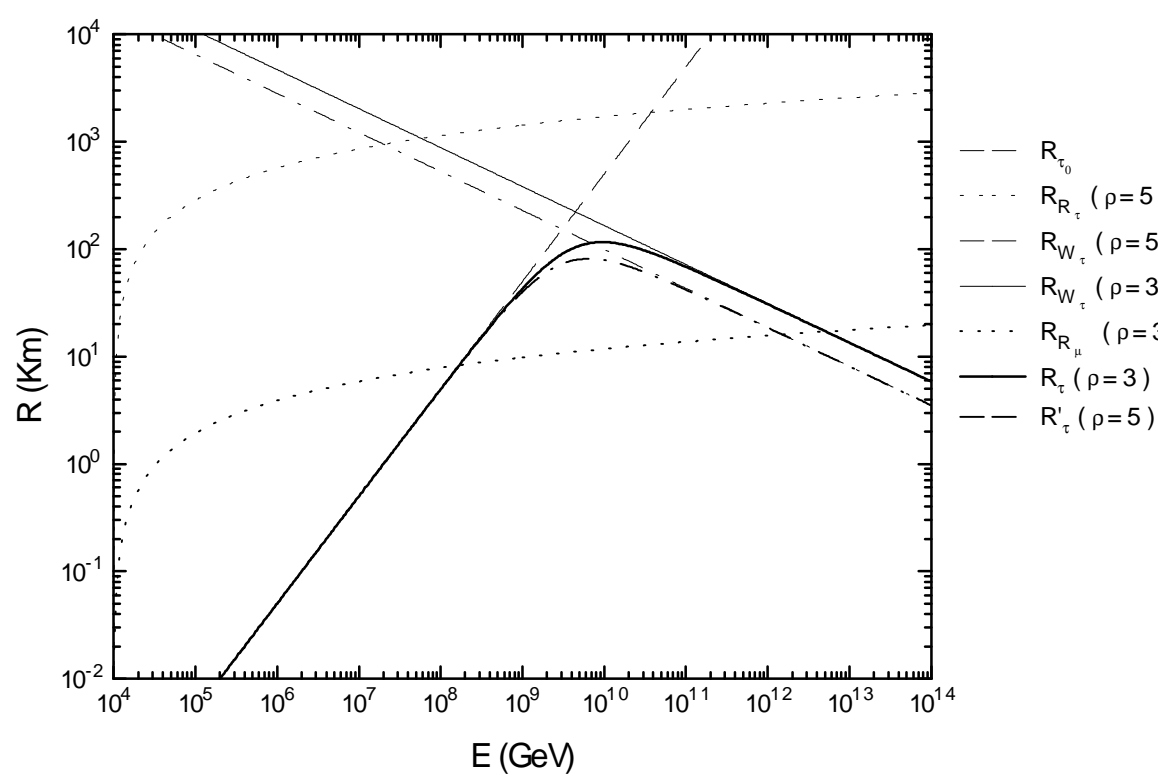
Fig. 13. Poisson probability distribution (and simulation) to find by chance  $N = (18)$  TGF events within 10 degrees from the galactic plane.

Fig. Table 1<sub>a</sub>.| BATSE terrestrial gamma burst data 1991-1999. The colored TGF events associate common arrival directions (Galactic Center, AGC center...) associated also in time clustering; the date, time, celestial coordinate, error bar, and TGF-Earth Center angle are listed below; Hard Trigger set up Trigger periods (channel 3+4) have a colored orange side label.

Fig. Table 1<sub>b</sub>.| BATSE gamma burst -GRBs- Trigger data 1991-1999 as a function of the Terrestrial Gamma Flash sequence. The different Trigger set up -Hard one for channel 3+4- are the root of the two evident plateau growth in TGF rate; colored TGF events associate common arrival directions -Galactic Center, AGC center...- related also in time clustering as in Table 1<sub>a</sub>.

Fig. Table 1<sub>c</sub>.| BATSE TGF rate 1991-1999. The diagram shows the inverse of the time lag between two consecutive TGF. The colored TGF events associate common arrival directions (Galactic Center, AGC center...) as in Table 1<sub>a</sub>; the inverse time lapse (inverse time interval between two sequential TGF events) marks the repeater nature of few TGF signals.

Fig. Table 2.| A Selected sample of very relevant Radio, X, TeV sources, their nature and arrival direction as in Figs 9-10, very possibly correlated to TGF events.



BATSE TERRESTRIAL GAMMA BURST 1991-1999							
N	Nº trigger	Date	Time	R.A.	Dec.	Δθ	Δθ geo
1	106	910422	2531, 1	99, 74	-11, 31	4, 42000	18.298
2	868	911005			Unpublished		
3	1300	920115	47202, 7	217, 85	-32, 34	16, 71000	50.007
4	1334	920201	72420, 0				
5	1433	920224	36547, 3				
6	1457	920301	81250, 8		Unpublished		
7	1470	920309	47072, 1	330, 568	-7, 418	3, 14600	27.240
8	1787	920810	61515, 2	305, 76	-47, 18	4, 26000	20.965
9	1915	920909	28074, 5	89, 59	-34, 33	5, 28000	39.621
10	2144	930124	54533, 6	205, 66	-25, 83	5, 59000	47.205
11	2185	930211	53095, 8	8, 4	26, 64	0, 23000	67.271
12	2221	930305	55291, 0	10, 84	64, 61	4, 73000	131.747
13	2223	930306	52583, 1	319, 652	-51, 879	0, 24893	51.343
14	2248	930315	60330, 1	59, 71	13, 27	0, 25000	151.511
15	2348	930520	7337, 7	281, 52	-16, 86	6, 15000	59.370
16	2370	930603	14440, 5	252, 45	-42, 27	6, 21000	24.210
17	2444	930712	50022, 5	127, 12	44, 73	7, 83000	35.895
18	2457	930723	18386, 9	312, 52	-51, 84	117, 33000	23.727
19	2465	930726	16888, 2	284, 41	-61, 57	6, 40000	38.168
20	2516	930905	79941, 0	244, 25	-27, 38	7, 19000	32.963
21	2573	931009	38648, 6	205, 96	11, 98	36, 38000	35.732
22	2692	931212	48679, 7	208, 722	16, 279	5, 97512	17.985
23	2754	940112	49046, 2	180, 72	-5, 97	8, 90000	55.155
24	2808	940209	22876, 9	215, 02	55, 15	0, 14000	44.431
25	2835	940219	58464, 9	323, 46	-13, 5	5, 49000	35.827
26	2955	940501	35887, 9	215, 49	41, 74	83, 37000	46.590
27	3148	940831					
28	3192	940925					
29	3233	941010					
30	3244	941016					
31	3258	941026					
32	3264	941030					
33	3274	941105					
34	3277	941109					
35	3285	941116					
36	3302	941127					
37	3309	941203					
38	3310	941203					
39	3313	941207					
40	3314	941208					
41	3315	941209					
42	3331	941228					
43	3377	950129	23619, 5	132, 94	7, 82	11, 79000	33.696
44	3382	950130					
45	3446	950228					
46	3457	950305					
47	3470	950316					
48	3474	950318					
49	3478	950321					
50	3500	950410					
51	3501	950410					
52	3813	950922	4147, 7	177, 363	-12, 77	8, 38576	51.854
53	3925	951128	25539, 1	306, 176	43, 554	9, 31987	52.484
54	3931	951204	55267, 1	189, 102	-0, 774	10, 23038	135.400
55	4355	960113	81867, 3	186, 553	29, 061	13, 82847	
56	5006	960224	67333, 9	278, 398	-8, 922	8, 50541	21.476
57	5317	960323	55341, 3	66, 203	26, 187	8, 12474	21.036
58	5520	960625	85244, 2	61, 958	-31, 575	11, 75859	46.283
59	5577	960817	13701, 4	88, 000	19, 354	11, 00976	32.485
60	5578	960817	46631, 7	75, 155	-10, 188	13, 80963	17.464
61	5579	960817	47563, 0	155, 715	7, 750	13, 28786	37.480
62	5582	960820	39893, 0	91, 151	29, 822	8, 91121	29.862
63	5583	960820	83982, 2	250, 510	-56, 233	469, 78418	116.460
64	5587	960827	74000, 9	245, 215	-48, 473	11, 66136	54.871
65	5588	960829	35537, 6	249, 631	-30, 47	7, 50174	29.902
66	5598	960909	42071, 1	336, 451	-27, 808	6, 35217	43.103
67	5665	961111	6460, 7	38, 713	69, 385	17, 44419	73.637
68	6185	970416	71107, 7	226, 787	12, 669	6, 25850	16.835
69	6773	980522	76751, 8	63, 817	44, 243	10, 37695	61.128
70	6777	980523	46630, 2	334, 484	-2, 996	6, 34613	31.810
71	7168	981021	57752, 1	146, 259	-34, 542	12, 68023	51.353
72	7208	981111	44176, 3	198, 714	-29, 859	5, 58169	27.523
73	7229	981125	44884, 9	303, 202	4, 903	2, 16981	54.592
74	7325	990114	53731, 0	120, 195	-16, 118	12, 77933	13.653
75	7844	991108	17993, 6	48, 525	19, 338	2, 09525	23.785

This figure "Tab01b.gif" is available in "gif" format from:

<http://arxiv.org/ps/astro-ph/0002453v3>

This figure "Tab01c.gif" is available in "gif" format from:

<http://arxiv.org/ps/astro-ph/0002453v3>

This figure "Fig02.gif" is available in "gif" format from:

<http://arxiv.org/ps/astro-ph/0002453v3>

X-Gamma Sources			TeV Source
Name	R.A.	Dec.	
Crab	83,52	22,19	A
Geminga	98,48	17,77	
PSR 1706-44	257,4	-44,52	A
PKS 0528	82,73	13,53	
PKS 2155-304	329,72	-30,22	B
Cyg X-3	308,11	40,96	
3C273	187,28	2,05	
3C279	194,05	-5,79	
Mrk 421	166,11	38,21	A
Vela X-1	135,28	-40,55	B
Virgo	187,5	13,2	
Omega - M 17	278	-10	
Perseo	49,96	41,53	
Coma	194	28	
Flys' Eye	87	48,1	
Mrk 501	253,47	39,76	A
Cen A	201,37	-43,02	
GRS 1915-105	289,33	10,55	
SCO X-1	244,98	-15,64	
RHO OPH	247,03	-24,54	
G.A. 1740-7-2942	266,01	-29,72	
Mrk 279	208,26	69,31	
GRO J2250-13	342,5	-13	
SN 1006	225	-41,5	B-
M31	10	40	
PKS 0235+164	39,66	16,61	
2EG J 0239+2818	40,09	28,21	
2EGS J0500+5902	75,15	59,04	
3C 454.3	343,49	16,13	
J0319+2407	49,76	24,12	
Her X-1	254,46	35,34	
PKS 1622-297	246,53	-29,86	
PKS 1959+650	300	65,08	B-

M31	Andromeda
	Unidentified
	Unmatched Sources
	Quasars or AGN
	PSR
	Galactic Center PSR
	Anti Galactic Center
	Nearby Quasars
	Nearby Galactic Clusters

This figure "Fig03a.jpg" is available in "jpg" format from:

<http://arxiv.org/ps/astro-ph/0002453v3>

This figure "Fig03b.gif" is available in "gif" format from:

<http://arxiv.org/ps/astro-ph/0002453v3>

This figure "Fig04.gif" is available in "gif" format from:

<http://arxiv.org/ps/astro-ph/0002453v3>

This figure "Fig05.gif" is available in "gif" format from:

<http://arxiv.org/ps/astro-ph/0002453v3>

This figure "Fig06.gif" is available in "gif" format from:

<http://arxiv.org/ps/astro-ph/0002453v3>

This figure "Fig07a.gif" is available in "gif" format from:

<http://arxiv.org/ps/astro-ph/0002453v3>

This figure "Fig07b.gif" is available in "gif" format from:

<http://arxiv.org/ps/astro-ph/0002453v3>

This figure "Fig08.jpg" is available in "jpg" format from:

<http://arxiv.org/ps/astro-ph/0002453v3>

This figure "Fig09.jpg" is available in "jpg" format from:

<http://arxiv.org/ps/astro-ph/0002453v3>

This figure "Fig10a.gif" is available in "gif" format from:

<http://arxiv.org/ps/astro-ph/0002453v3>

This figure "Fig10b.jpg" is available in "jpg" format from:

<http://arxiv.org/ps/astro-ph/0002453v3>

This figure "Fig11.gif" is available in "gif" format from:

<http://arxiv.org/ps/astro-ph/0002453v3>

This figure "Fig12.gif" is available in "gif" format from:

<http://arxiv.org/ps/astro-ph/0002453v3>

This figure "Fig13.gif" is available in "gif" format from:

<http://arxiv.org/ps/astro-ph/0002453v3>